Critical feature and seawater testing of cross-flow rotor components fabricated with additive manufacturing

James R. McVey, Robert J. Cavagnaro, John T. Zaengle, Michelle D. Fenn, Christopher R. Rumple, and Brittnee E. Lommers

Abstract—**Cross-flow tidal turbines may be a viable option for providing power at sea and to remote communities, but the geometry of these rotors can prove difficult to manufacture with traditional methods. Additive manufacturing (AM) offers an opportunity to print rotor geometries that are lighter, stronger and less expensive to produce, as well as in a variety of materials that could be useful for marine energy applications. In this study, AM materials were categorized into 3 classes – plastics, metals, and ceramics – and reviewed for suitability based on a set of engineering requirements and criteria. Two plastics and two metals were selected to undergo further testing: Essentium CF25, Markforged Onyx, titanium Ti-6Al-4V, and Inconel 718. Dogbone-shaped specimens were printed in each material and divided into two test groups. The first group was tensile tested, as printed, to get a material baseline. The second was tensile tested after being submerged in seawater tanks for 6 months to determine water uptake, corrosion, and biofouling resistance. While little macroscopic change and water uptake were observed after seawater testing, tensile testing of the plastic materials showed significant degradation, with losses in strength between 30% and 50%. Conversely, printed metal materials showed little to no decrease in strength. Future fatigue and flume testing will focus on the metals, as these materials show promising performance for marine energy use cases.**

Index Terms—**Additive Manufacturing, Environmental Degradation, Marine Energy**

I. Introduction

CROSS-FLOW hydrokinetic turbines (e.g., Fig. 1) are an attractive option for powering remote loads or community-scale applications compared to axial-flow devices due to their relative simplicity and other unique characteristics. They typically have a single degree of freedom, not requiring blade pitching or yawing mechanisms and when oriented vertically, can harvest power from any current direction. Lift-based designs utilize foil profiles with smooth surface finish for blades, which generate the hydrodynamic forces resulting in power generation. Design variation exists in blade count, profile, shape (e.g., straight, helical, or troposkein) and support structure, though all designs share the characteristics of requiring a means by which to attach blades from their radial extent to a central shaft for power transfer and support [1]. A high-stress connection on the turbine, this joint is subjected to rotating force vectors and fatigue. Variation exists in this connection mechanism, which may be a plate, endcap, or struts. The positioning and shape this blade connection has a significant impact on turbine performance and these features must be designed for efficient power generation and structural stability [2]. Similarly, surface properties of blades impact performance and structural loading, with aberrations like barnacle growth causing degradation [3].

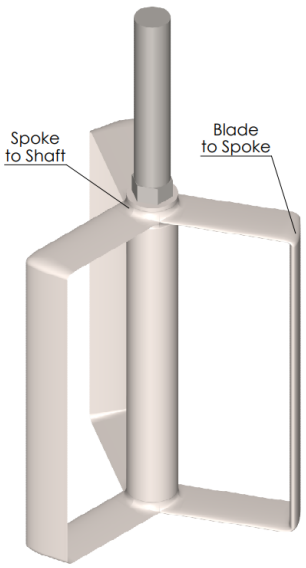

Fig. 1. Conceptual 3-bladed cross-flow turbine with printed blade to spoke and spoke to shaft connections

Additive manufacturing (AM) offers an opportunity to rapidly fabricate complex parts from polymeric, composite, or metallic feedstock that can result in components that may be lighter, stronger, more corro-

This work was authored by the Pacific Northwest National Laboratory, operated by Battelle Memorial Institute for the U.S. Department of Energy (DOE) under Contract No. DE-AC05-76RL01830. Funding provided by the U.S. Department of Energy Office of Energy Efficiency and Renewable Energy Water Power Technologies Office. The views expressed herein do not necessarily represent the views of the DOE or the U.S. Government. The U.S. Government retains and the publisher, by accepting the article for publication, acknowledges that the U.S. Government retains a nonexclusive, paid-up, irrevocable, worldwide license to publish or reproduce the published form of this work, or allow others to do so, for U.S. Government purposes.

J.R. McVey, R.J. Cavagnaro, and C.R. Rumple are with the Coastal Sciences Division, Pacific Northwest National Laboratory, 1529 W Sequim Bay Rd, Sequim, WA 98382 U.S.A (e-mail: james.mcvey@pnnl.gov).

J.T. Zaengle, M.D. Fenn, and B.E. Lommers are with the National Security Division, Pacific Northwest National Laboratory, 902 Battelle Blvd, Richland, WA 99354 U.S.A.

Digital Object Identifier:
https://doi.org/10.36688/ewtec-2023-222

sion resistant, and/or less expensive to produce than traditional manufacturing techniques [4]. Though revolutionary for manufacturing, the renaissance of AM has resulted in a wide variety of printing processes, techniques and materials which must be reviewed or investigated for suitability to each application. For example, material fatigue performance, critical for components with high degrees of cyclic loading, is generally poorer than traditional manufacturing techniques for polymers printed using fused deposition modeling (FDM) methods and depends on parameters including raster angle and build orientation [5].

Additive manufacturing is increasingly being used to fabricate renewable energy technologies, such as wind turbine parts, due to its ability to create unique geometries and to enable rapid design iteration [6]. While many applications of AM in wind energy are focused on prototype development to support large-scale designs, it has been demonstrated that it is feasible to print many components of a cross-flow wind turbine at a scale appropriate for emergency scenarios and rural electrification [7]. Similarly, AM techniques for composite materials have shown promise in the construction of marine hydrokinetic turbines through the creation of blade molds or internal blade structures [8]. However, differences in performance characteristics, including power and thrust between turbine rotors printed of polymers (e.g., nylon) and those conventionally machined in aluminum, have been shown, with performance degradation attributed to material flexibility [9].

We posit that the distinct characteristics of cross-flow turbines align well with the capabilities and advantages of AM processes and materials. In particular, the ability to print blade-strut and strut-shaft joints as one part, avoiding bonded, bolted, pinned, or welded connections at high stress points on the turbine, is motivation for this investigation. Herein, we review prospective materials relevant to cross-flow turbine fabrication and describe preliminary testing of their as-printed properties for strength and ability to withstand continued immersion in seawater – key for determining ultimate suitability for the application. Finally, we discuss follow-on work to characterize turbine efficiency and gauge the impact of materials and print parameters on fatigue performance.

II. Methods

A. Material Selection

The proliferation of AM as a widely-used technology has resulted in a landscape where dozens of processes, printers, and material formulations are available for designers to choose from for a given application. To narrow our focus on a preliminary feasibility study, we consider a design objective of manufacturing the majority of components for or an entire miniature cross-flow tidal turbine with characteristic dimensions (diameter and height) on the order of 20 cm. Such a turbine would be capable of generating tens of W in flow of 1-2 m/s, suitable for powering oceanographic sensors for sustained observations [10]. A list of design criteria was established to compare specific printers/materials qualitatively using the technique of a Pugh chart, in which a datum option is chosen and alternatives are rated on a relative scale and subject to weightings established to emphasize relative importance of criteria. The criteria ultimately utilized in the analysis of the materials, listed in order from highest to lowest weighting, were fatigue life/limit, strength to weight ratio, corrosion resistance, toughness, elastic modulus, water uptake, surface finish, cost of material, cost to print, and biofouling potential. Print methodology was also considered to understand scalability by comparing, again in order of importance, print volume, print resolution, print location (i.e. in-house at PNNL vs. external), and time to print. Of 29 materials identified as potentially viable, 7 were plastics, 17 were metal alloys, and 5 were ceramic materials. The full list of materials was narrowed down to 5 plastics and 3 metal alloys for consideration of design criteria in the Pugh chart analysis. The ceramic materials and most metals were dropped from the Pugh chart analysis because of their brittleness and lack of availability, respectively. The remaining materials were scored relative to a datum representing a standard manufacturing process and material: CNC-machined 6061 aluminum alloy. The top two plastics and metals were selected to undergo experimental evaluation.

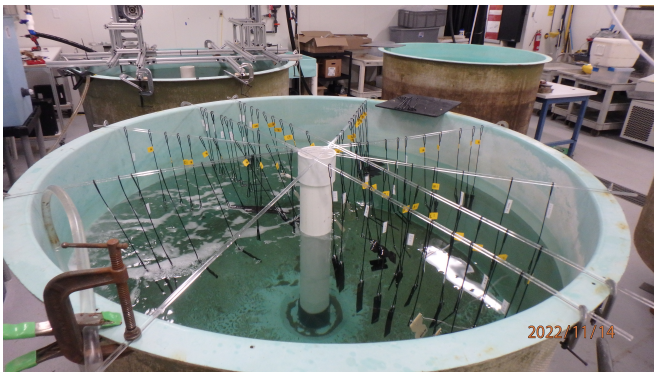

Fig. 2. Samples undergoing environmental conditioning suspended in a seawater tank in PNNL-Sequim

The two plastics chosen for testing were Essentium HTN-CF25 and Markforged Onyx. Both are high-temperature nylons with carbon fiber reinforcement, which have high strength, toughness, and chemical/heat resistance compared to other plastic filament materials. Nylon is shown to have relatively high strength for a polymeric material while maintaining flexibility, which makes it an ideal candidate for cyclic applications [11]. These materials were printed using desktop FDM printers.

Essentium HTN-CF25 is a nylon-based filament with a 25% carbon fiber-reinforced core. Essentium claims an ultimate tensile strength (UTS) of 148 MPa; although, this UTS is achieved only when the infill angle is oriented parallel to the active load (i.e. the carbon fiber based core is in line with the active load). When the infill angle is perpendicular with the pulling force, the tensile strength decreases to 40 MPa. Markforged Onyx improves the strength of nylon through the

addition of chopped carbon fiber mixed into the entire volume of the filament, rather than only in the core. Onyx claims a tensile strength of 40 MPa.

Titanium (Ti-6Al-4V) and Inconel 718 were the metal materials selected and are both made using direct metal laser sintering (DMLS). This is an industrial printing process where a laser sinters/welds metal powder together to form the 3D part. Titanium Ti-6Al-4V was chosen because of its high strength-to-weight ratio and superior corrosion resistance. Inconel 718, a nickel-chromium alloy, was chosen for the same reasons, although it is stronger, stiffer, denser, and slightly more expensive than titanium. When weight is a factor, titanium is the better option, and when absolute strength is a consideration, Inconel is preferred. The DMLS process allows these materials, which traditionally are difficult to form, to be considered for this application. The third metal, 316 stainless steel, and the datum, 6061 aluminum, were not selected for this analysis because they are more susceptible to corrosion and have lower strength than the chosen metals.

B. Tensile and Seawater Testing

Testing was conducted to determine the 3D printed material performance for two of the top design criteria (strength and corrosion resistance), comparing properties before and after a prolonged immersion in seawater. Six total dogbone samples were printed of each material, and testing was conducted in three phases: a pre-seawater exposure tensile test, seawater exposure (i.e., environmental conditioning), and a post-seawater exposure tensile test. These tests were designed to discern the suitability of these AM materials since their properties from 3D printing processes are known to vary from published parameters, as well as to analyze material degradation after exposure to untreated seawater.

Plastic dogbone samples were printed in-house at PNNL-Richland on a Markforged Mark Two FDM printer with 100% (solid) infill, 2 wall layers, and a layer height of 0.1 mm. The metal dogbones were ordered from Protolabs, an online-based vendor, and printed on a GE Additive M2 DMLS printer with a layer height of 30 microns. Dogbone shapes were determined from the appropriate standard for each material: ISO 527 for the plastic materials and ASTM E8 for the metal alloys. The longest dogbone dimension was scaled to 75 mm for the plastic coupons and 100 mm for the metal coupons. For the first phase of testing, three dogbones of each material were tensile tested at the PNNL-Richland Mechanical Test Lab on an Instron 5582 load frame. The metal dogbones were tested in accordance with ASTM E8 standard, using a 30 kN load cell and a 13.3 N preload. The plastic dogbones were tested in accordance with the ISO 527, Type 1BA standard, using a 5 kN load cell and a preload of 10 N, and were loaded at a strain rate of 0.45 mm/min until failure. This initial set of tensile testing established a baseline to compare the Young's modulus of the printed materials to published values. Other material properties, such as ultimate tensile strength (UTS) and maximum elongation or strain, are functions of the material fabrication process (e.g. hot- vs cold-worked, annealing temperature, etc) and therefore aren't directly comparable.

Fig. 3. Post seawater immersion: Onyx (a.), Essentium (b.), Titanium (c.) and Inconel (d.)

Next, three additional samples of each material were immersed in seawater tanks at PNNL-Sequim to study corrosion, water uptake, and biofouling potential. Untreated seawater was pumped from Sequim Bay, WA to a 1.5 m deep by 1.6 m diameter cylindrical fiberglass tank. The volume of these tanks was cycled through every 12 hours.

Printed coupons were hung with plastic clips attached with a twine neoprene loop to acrylic rods spanning the lid of the tank to prevent galvanic corrosion between samples, and are shown in Fig. 2. Before environmental conditioning, samples were labeled and weighed to the nearest 0.1 g. Samples were conditioned for 6 months from November 14, 2022 to April 20, 2023, with photos taken each month to document any progression of corrosion and biofouling. It should be noted that due to project timing, environmental conditioning was conducted over the winter months, when marine growth rates are their slowest.

After the test period was completed, samples were removed and photographed prior to cleaning to show the ultimate extent of biofouling coverage and corrosion, if any. Samples were wiped clean with a cloth towel to remove any growth and residual surface moisture and weighed a second time. They then underwent identical tensile testing as the pre-seawater exposure samples to quantify the effects of seawater on the materials.

III. Results

The chosen materials were known to be particularly resistant to corrosion, and they showed no corrosion

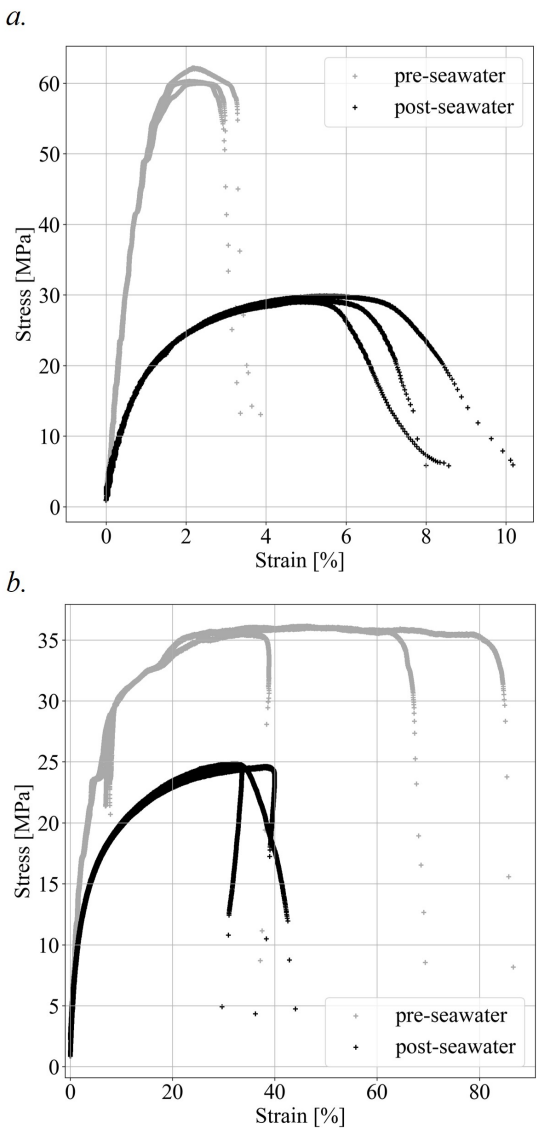

Fig. 4. Essentium (a.) and Oynx (b.) stress-strain curves. Pre-seawater sample curves are in gray, and post-seawater test sample curves are in black.

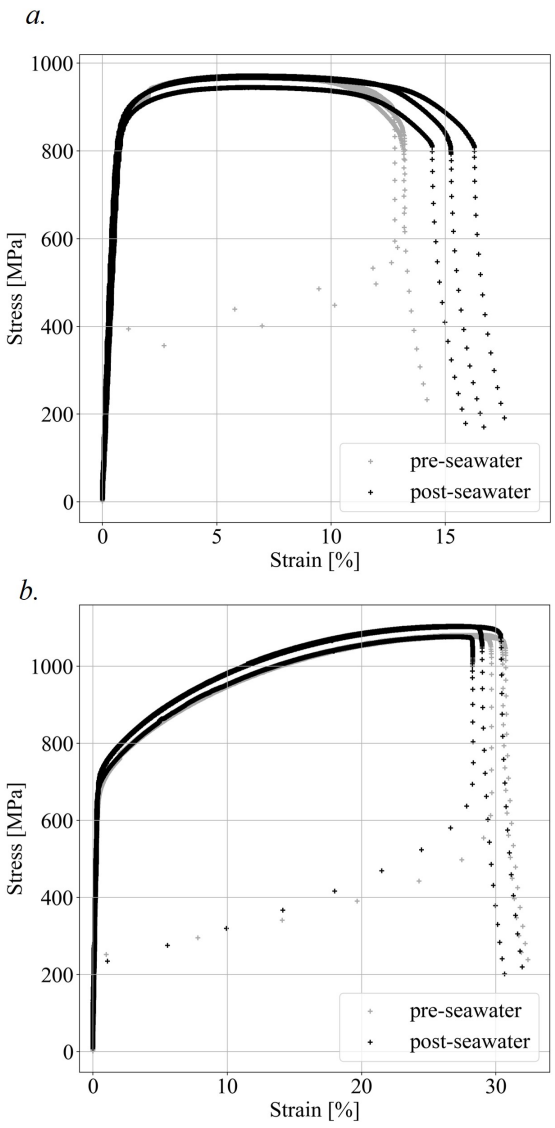

Fig. 5. Titanium (a.) and Inconel (b.) stress-strain curves. Pre-seawater sample curves are in gray, and post-seawater test sample curves are in black.

TABLE I
ESSENTIUM RESULTS

	Pre-Seawater	Post-Seawater	Change
Elastic Modulus [MPa]	6,920	2,164	-68.7%
UTS [MPa]	60.8	29.4	-51.7%
Load at UTS [N]	607.4	322.3	-46.9%
Max Strain [%]	3.62	8.92	146%
Sample Weight [g]	1.2	1.3	8.3%

TABLE II
ONYX RESULTS

	Pre-Seawater	Post-Seawater	Change
Elastic Modulus [MPa]	2,450	685	-72.0%
UTS [MPa]	35.9	24.8	-31.0%
Load at UTS [N]	358.6	234.2	-34.7%
Max Strain [%]	65.0	39.2	-39.7%
Sample Weight [g]	1.2	1.2	0.0%

and no visual biofouling (as expected for testing in cooler months) after 155 days of exposure. Fig. 3 shows one sample from each of the four materials.

While few visual indications of corrosion or degradation were observed after seawater exposure, tensile tests of these samples showed that the plastic samples weakened after 155 days of submersion. The Essentium samples, shown in Fig. 4a, have drastically changed material properties. In the post-seawater samples, little elastic deformation was observed and they quickly transition to plastic deformation until their breaking point (29 MPa) at around 50% of their original (pre-seawater) strength (60 MPa). Similarly, max strain more than doubles between the original and post-seawater samples (3% vs 8%). The weight difference between before and after submersion testing was 0.1 g, or 8.3%. The material properties before and after seawater tank testing for the Essentium dogbones are shown in Table I.

The post-seawater Onyx samples show a decrease in both ultimate strength and strain when compared to the pre-seawater samples, though not as drastic as the

TABLE III
TITANIUM (TI-6AL-4V) RESULTS

	Pre-Seawater	Post-Seawater	Change
Elastic Modulus [MPa]	121,600	121,500	-0.1%
UTS [MPa]	968.8	960.8	-0.8%
Load at UTS [N]	12,170	12,250	0.7%
Max Strain [%]	13.4	16.7	24.7%
Sample Weight [g]	8.0	8.0	0.0%

TABLE IV
INCONEL 718 RESULTS

	Pre-Seawater	Post-Seawater	Change
Elastic Modulus [MPa]	205,000	182,500	-10.9%
UTS [MPa]	1078.	1094.	1.5%
Load at UTS [N]	13,520	13,830	2.3%
Max Strain [%]	31.3	30.3	-3.2%
Sample Weight [g]	14.5	14.6	0.7%

Essentium specimens. Ultimate tensile strength (UTS) decreased 31% from 35 MPa to 25 MPa and max strain is reduced from 65% to 39% after seawater exposure. Material property changes, averaged across all three samples, are shown in Table II. One of the original Onyx samples slipped in the test apparatus, resulting in a drop of 10 MPa at a strain rate of 7%, reaching the same UTS but 30-40% lower strain than that measured for the other two specimens. Little water uptake was measured for the Onyx samples; the average change for the 3 specimens was 0.0 g.

The metal materials show little change (less than 3%) between the original and post-seawater testing samples, seen in Fig. 5. Both titanium and Inconel stress-strain curves remained consistent through elastic deformation until reaching yield, where there is some variation between samples. After seawater exposure, the elastic modulus changed less than 1% for titanium, though it decreased 10% for the Inconel samples. The titanium samples overall had a higher yield strength than the Inconel samples, although the UTS of Inconel is higher than titanium. Intriguingly, the maximum strain of the titanium specimens increased 25% post-seawater exposure as compared to the pre-seawater samples, though additional testing would be needed to confirm this result. Average material properties are shown in Tables III and IV for titanium and Inconel, respectively. Comparisons between the published elastic modulus and that measured from the pre-seawater samples for both metals are shown in Table V. The AM titanium and Inconel have a similar but slightly higher elastic modulus than their traditionally manufactured counterparts at 6.9% and 2.8%, respectively (at room temperature).

IV. DISCUSSION & CONCLUSIONS

Significant degradation was seen in the nylon-based printed material samples after seawater exposure, which was somewhat surprising given that nylon rope is commonly used in the maritime industry and does not experience the degradation seen here [14]. While composite materials are used successfully in the marine environment [15], carbon-plastic composites have been shown to degrade significantly in seawater due to debonding and delamination of the fiber from the matrix [16], [17]. Essentium and Onyx, as printed in this study, are not "true" composites since they do not contain continuous fibers running through the nylon matrix; rather, carbon particles are blended into the nylon filament itself. Regardless, it appears possible that the loss in strength of the nylon materials is due to the same debonding mechanism that degrades "true" composites: water molecules diffuse into the material through pore spaces and break the bond between the nylon molecules and carbon atoms (i.e. hydrolysis) [17]. This could be confirmed in future studies through analysis of samples using microscopy.

TABLE V
PUBLISHED VERSUS ADDITIVE ELASTIC MODULI FOR METAL MATERIALS

	Published [MPa]	Pre-Seawater [MPa]	Difference
Titanium	113,800 [12]	121,600	6.9%
Inconel	199,950 [13]	205,000	2.8%

Differences in the behavior of Essentium and Onyx are possibly due to how carbon fiber particulates are distributed in the material. Since the carbon fiber in Essentium is concentrated in the core of the fiber, the increased pliability of the material is due to the nylon molecules "freed" from the carbon core, while the increased brittleness of the Onyx is likely caused by bonds broken throughout the material, rather than just the core. In either case, it is recommended that future studies of 3D-printed FDM materials in seawater should focus on non-reinforced polymeric materials to avoid hydrolysis of the material.

Titanium and Inconel perform as expected after seawater testing, with little change in material properties, except for the 25% increase in maximum strain of the titanium samples and the 10% decrease in the Inconel specimens' elastic moduli. Both warrant further investigation as the reasons for the increase in maximum elongation and decrease in elastic modulus for titanium and Inconel, respectively are difficult to speculate on. The elastic moduli of each of the AM version of these materials is higher than published parameters, which means the AM versions have greater resistance to elastic deformation than expected, a positive for turbine rotors. While the Inconel samples' elastic modulus decreased after seawater testing, the shear magnitude of Inconel's is greater than the titanium's samples. The tradeoff between Inconel and titanium still remains titanium's lower density, as greater rotor inertia will translate to greater torque on a turbine's PTO.

The lack of macro-biofouling on any of the four materials tested can be attributed mainly to the timing of testing which occurred primarily over the winter months, where decreased sunlight and colder temperature prohibits marine growth [18]. Biofouling is geographically specific, and it was only during the last

month of testing (April, 2023) that growth was seen on other samples in adjacent seawater tanks unaffiliated with this experiment, and more work is needed to fully study biofouling resistance.

The poor material properties of Essentium and Onyx after seawater immersion likely renders them unsuitable for use in the marine environment, particularly in high-stress applications like turbine rotors, where resilience is key to performance. Titanium Ti-6Al-4V and Inconel 718 are two metals that have been used successfully in the marine environment and demonstrated retention of their strength even in 3D-printed form.

Future work is focused on two avenues: the first is investigating fatigue performance to understand how print orientation and design affect the critical features of interest; the second is measuring the performance characteristics and blade strain of rotors constructed using the promising materials in a laboratory flume.

ACKNOWLEDGEMENT

The authors thank Rob Seffens and Tim Roosendaal for running tensile tests at the PNNL-Richland Mechanical Test Lab and Protolabs for creating the metal specimens used in this study. Seawater tank testing was conducted in the PNNL-Sequim Wet Labs.

REFERENCES

[1] G. Saini and R. P. Saini, "A review on technology, configurations, and performance of cross-flow hydrokinetic turbines," *International Journal of Energy Research*, vol. 43, no. 13, pp. 6639–6679, 2019.

[2] B. Strom, N. Johnson, and B. Polagye, "Impact of blade mounting structures on cross-flow turbine performance," *Journal of Renewable and Sustainable Energy*, vol. 10, no. 3, p. 034504, 2018.

[3] C. C. Stringer and B. L. Polagye, "Implications of biofouling on cross-flow turbine performance," *SN Applied Sciences*, vol. 2, pp. 1–13, 2020.

[4] A. Paolini, S. Kollmannsberger, and E. Rank, "Additive manufacturing in construction: A review on processes, applications, and digital planning methods," *Additive manufacturing*, vol. 30, p. 100894, 2019.

[5] V. Shanmugam, O. Das, K. Babu, U. Marimuthu, A. Veerasimman, D. J. Johnson, R. E. Neisiany, M. S. Hedenqvist, S. Ramakrishna, and F. Berto, "Fatigue behaviour of FDM-3D printed polymers, polymeric composites and architected cellular materials," *International Journal of Fatigue*, vol. 143, p. 106007, 2021.

[6] M. N. Nadagouda, M. Ginn, and V. Rastogi, "A review of 3D printing techniques for environmental applications," *Current opinion in chemical engineering*, vol. 28, pp. 173–178, 2020.

[7] K. Bassett, R. Carriveau, and D.-K. Ting, "3d printed wind turbines part 1: Design considerations and rapid manufacture potential," *Sustainable Energy Technologies and Assessments*, vol. 11, pp. 186–193, 2015.

[8] P. Murdy, J. Dolson, D. Miller, S. Hughes, and R. Beach, "Leveraging the advantages of additive manufacturing to produce advanced hybrid composite structures for marine energy systems," *Applied Sciences*, vol. 11, no. 3, p. 1336, 2021.

[9] P. Liu, N. Bose, R. Frost, G. Macfarlane, T. Lilienthal, and I. Penesis, "Model testing and performance comparison of plastic and metal tidal turbine rotors," *Applied Ocean Research*, vol. 53, pp. 116–124, 2015.

[10] R. Green, A. Copping, R. J. Cavagnaro, D. Rose, D. Overhus, and D. Jenne, "Enabling power at sea: Opportunities for expanded ocean observations through marine renewable energy integration," in *OCEANS 2019 MTS/IEEE SEATTLE*, 2019, pp. 1–7.

[11] N. G. Tanikella, B. Wittbrodt, and J. M. Pearce, "Tensile strength of commercial polymer materials for fused filament fabrication 3D printing," *Additive Manufacturing*, vol. 15, pp. 40–47, 2017.

[12] MatWeb. Titanium Ti-6Al-4V (Grade 5), Annealed. [Online]. Available: https://www.matweb.com/search/datasheet.aspx?MatGUID=a0655d261898456b958e5f825ae85390

[13] Special Metals Inconel 718. [Online]. Available: https://www.specialmetals.com/documents/technical-bulletins/inconel/inconel-alloy-718.pdf

[14] M. Kenney, J. F. Mandell, and F. McGarry, "The effects of sea water and concentrated salt solutions on the fatigue of nylon 6, 6 fibres," *Journal of materials science*, vol. 20, pp. 2060–2070, 1985.

[15] A. P. Mouritz, E. Gellert, P. Burchill, and K. Challis, "Review of advanced composite structures for naval ships and submarines," *Composite structures*, vol. 53, no. 1, pp. 21–42, 2001.

[16] A. Siriruk and D. Penumadu, "Degradation in fatigue behavior of carbon fiber–vinyl ester based composites due to sea environment," *Composites Part B: Engineering*, vol. 61, pp. 94–98, 2014.

[17] S. Koshima, S. Yoneda, N. Kajii, A. Hosoi, and H. Kawada, "Evaluation of strength degradation behavior and fatigue life prediction of plain-woven carbon-fiber-reinforced plastic laminates immersed in seawater," *Composites Part A: Applied Science and Manufacturing*, vol. 127, p. 105645, 2019.

[18] G. D. Bixler and B. Bhushan, "Biofouling: lessons from nature," *Philosophical Transactions of the Royal Society A: Mathematical, Physical and Engineering Sciences*, vol. 370, no. 1967, pp. 2381–2417, 2012.